Physical aspects of cardiac magnetic fields and electric potentials

O. Kosch, P. Meindl, U. Steinhoff and L. Trahms

Physikalisch-Technische Bundesanstalt, Berlin, Germany

1 Introduction

Current sources in the myocardium can be investigated by measurements of the electrical potential and magnetic field components. Franzone [1] has pointed out the importance of anisotropy and inhomogeneity of the conductivity in the cardiac tissue. In this paper we describe some principle influences of these structures on the electrical and magnetic field in several simple configurations. Based on the theory of electromagnetic field we show some differences between the information content of ECG and MCG and their dependence on the current source configuration.

2 Methods

2.1 Forward calculation for half space

To investigate the influence of strong anisotropic conductivity we have analyzed the electrical potential and magnetic field for a straight and a curved line source. To this end we have employed analytical field calculations for infinite half space geometry.

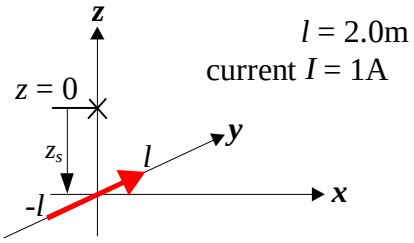

Figure 1: *Configuration of the straight line source*

The used conductivity for $z < 0$ is $\kappa = 0.2$ S/m and zero in the upper half space. In infinite space the electrical potential at a point P($\vec{r}$) of a line source is given by

$$\varphi(\vec{r}) = \frac{I}{4\pi\kappa} \cdot \int_{-l}^{l} \frac{(\vec{r} - \vec{r}_s)d\vec{s}}{\left|\vec{r} - \vec{r}_s\right|^3}, \qquad (1)$$

where $\vec{s}$ is the path of the line source and $\vec{r} - \vec{r}_s$ the distance vector between line source and the point P. Taking into account the boundary of the half space at $z = 0$ the electrical potential of the straight line source at $x_s = 0$, $-l < y_s < l$, z_s becomes for the boundary plane Eq. 2.

$$\varphi(x,y,0) = \frac{I}{2\pi\kappa} \cdot \left[\frac{1}{\sqrt{x^2 + (y - y_s)^2 + z_s^{\,2}}} \right]_{y_S=-l}^{y_S=l} \qquad (2)$$

The magnetic field density of a line source can be obtained with Biot-Savart's law

$$\vec{B}(\vec{r}) = \frac{\mu I}{4\pi} \cdot \int_{-l}^{l} \frac{d\vec{s} \times (\vec{r} - \vec{r}_s)}{\left|\vec{r} - \vec{r}_s\right|^3} \qquad (3).$$

The B_z component of the straight line source at $x_s = 0$, $-l < y_s < l$, z_s is not influenced by the boundary and described at $z = 0$ by

$$B_z(x,y,0) = \frac{\mu I}{4\pi} \cdot \left[\frac{-(y - y_s)}{(x^2 + z_s^2)\sqrt{x^2 + (y - y_s)^2 + z_s^{\,2}}} \right]_{y_s=-l}^{y_s=l} \qquad (4).$$

The integration parameter in the solution of the curved line source is the angle α_s with a constant radius R.

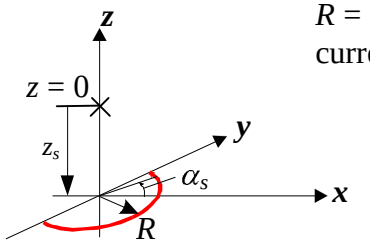

Figure 2: *Configuration of the curved line source*

The electric potential at the boundary plane ($z = 0$) with the curved line source is given by

$$\varphi(x,y,0) = \frac{I}{2\pi\kappa} \cdot \left[\frac{1}{R\sqrt{R^2 + r_1^2 - 2R\,(x\cos\alpha_s - y\sin\alpha_s)}} \right]_{\alpha_S=-\frac{\pi}{2}}^{\alpha_S=\frac{\pi}{2}} \qquad (5)$$

where $r_1^2 = x^2 + y^2 + z_s^2$ is the quadratic distance between the center of the curved line source and the point P. The B_z component of the magnetic flux density was calculated by numerical integration of Eq. 3.

2.2 Numerical simulation with a torso model

Furthermore, we have calculated numerically the electric potential and magnetic field components using a boundary element model of the human torso with 434 nodes [2]. The conductivity is assumed to be the same as in the analytical calculation. The B_z component of the magnetic flux density is calculated in two arrays of 9x9 positions. One is placed in front and the other on back side of the torso.

The electrical potential is determined in the 434 nodes of the torso.

3 Results

3.1 Straight line source in half space

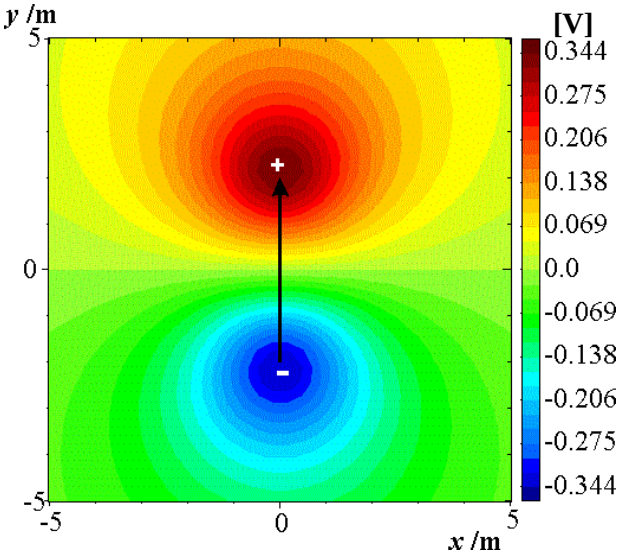

Figure 3: *Mapping of the electrical potential φ at the boundary plane of the straight line source (distance between source and plane 1.5m)*

The map of the electric potential of the straight line source looks very similar to the field of a single current dipole. The difference to the dipole field can be described by the field of an electrical octupole [3] which decreases rapidly with the distance from the source. Thus, a single dipole in a straight muscle fiber with anisotropic conductivity produces in some distance from the source an electric potential very similar to isotropic conditions.

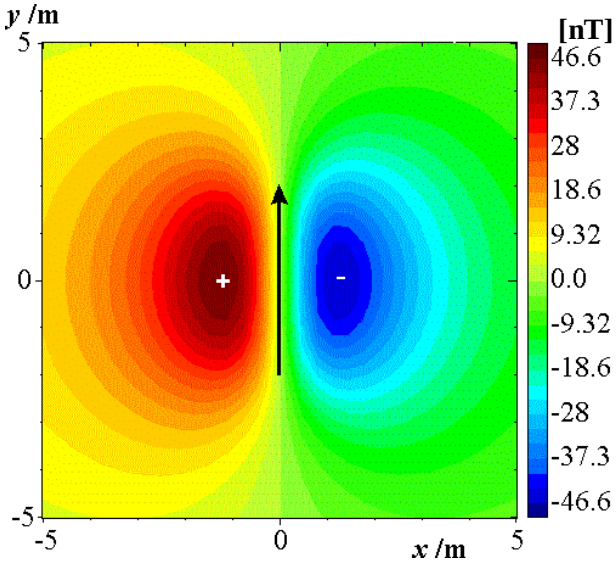

Figure 4: *Mapping of the B_z component of the straight line source in the x-y-plane in a distance of 2.5m in z- direction*

The distribution of the magnetic B_z component due to the straight line source shown in Fig. 4 is symmetric, but, with respect to the field of a single dipole, stretched in the direction of the source extension. This effect depends on the length of the line source and increases with the source extension.

3.2 Curved line source in half space

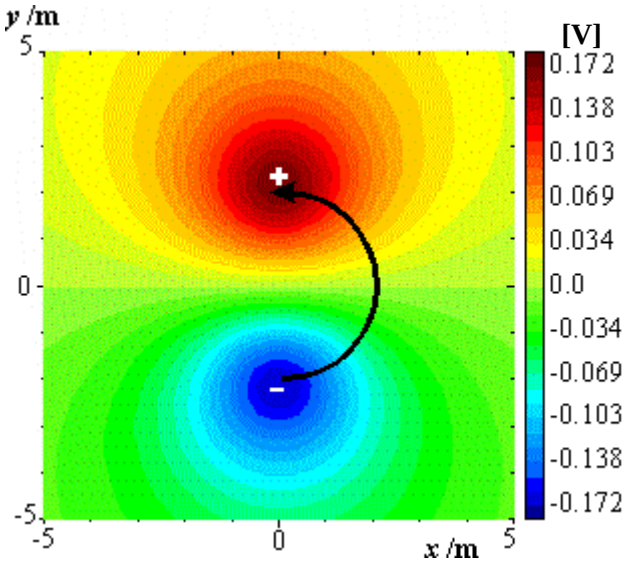

Figure 5: *Mapping of the electric potential φ at the boundary plane of the curved line source (distance between source and plane 1.5m)*

The potential distribution of the curved line source is identical to that of a straight line source, but the amplitude decreased by factor two.

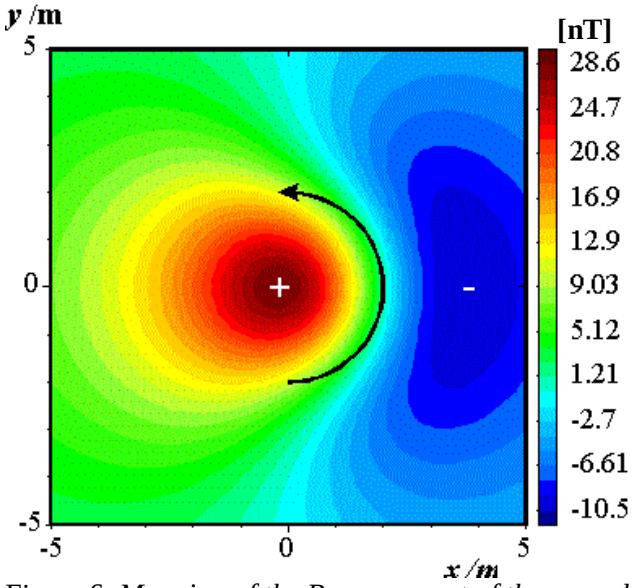

Figure 6: *Mapping of the B_z component of the curved line source in the x-y-plane in a distance of 2.5m in z-direction*

The field of the magnetic B_z component of a curved line source is clearly non-symmetric. It shows a flux density concentration above the center of the curvature, and a smaller spread extremum at the outside.

3.3 Simulations with a BEM model and comparison to measurements

Simulations with a BEM model were carried out in order to estimate the additional effects of the volume currents. The results were compared to measured field and potential distributions [4].

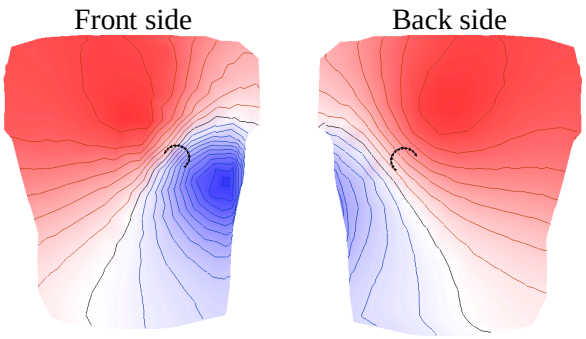

Figure 7: Simulated distribution of the electrical potential on the thorax (1 isoline means 0.1V)

The potential distributions generated by straight and curved line sources were identical, equivalent to the analytical calculations. By manually changing the source parameters, we have found a potential distribution (Fig. 7) that is similar to the measured potential distribution in Fig. 8.

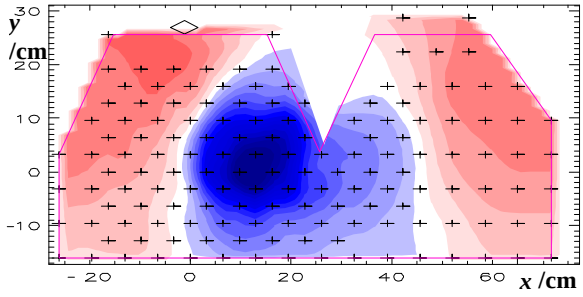

Figure 8: Measured distribution of the electrical potential during the QRS complex (1isoline = 0.1V)

The distribution of the magnetic B_z component calculated with the BEM model show difference between the straight line source and the curved line source.

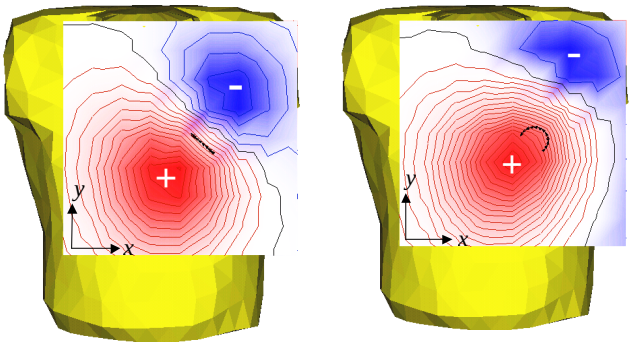

Figure 9: Simulated distribution of the magnetic B_z component during the QRS complex at the front side of the thorax (1isoline = 2 pT).

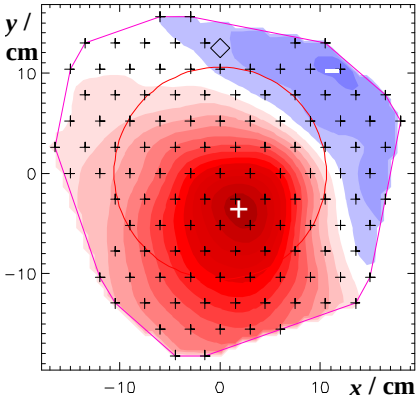

Figure 10: Measured distribution of the magnetic B_z component during the QRS complex at the front side of the thorax (1isoline = 2 pT).

In contrary to the analytical case, the field produced by a straight line source is not symmetrical, due to the influence of the volume currents. That effect is

growing up if the source is closer to the boundary of the volume conductor. The field of the curved line source exhibits a distributed minimum. The highest field gradient is located above the source, but the zero line is curved and shifted towards the negative extremum. While the measured potential distribution can be explained by both a straight or a curved line source, the measured magnetic field is better described by the curved line source model. This difference is also recognizable at the back side of the thorax, but the differences between the two BEM simulations are smaller, due to the larger influence of the volume conductor in regions further away from the source.

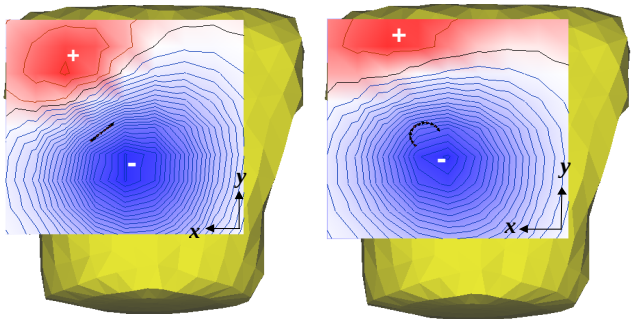

Figure 9: Simulated distribution of the magnetic B_z component during the QRS complex at the back side of the thorax (1isoline = 2 pT).

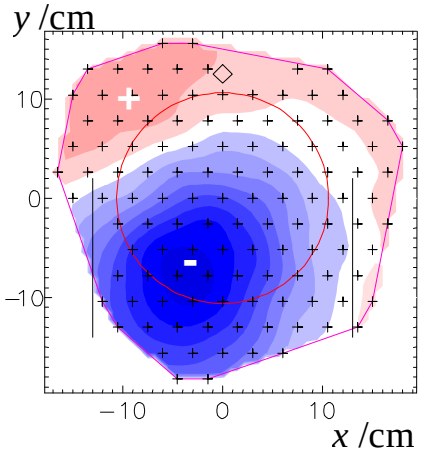

Figure 10: Measured distribution of the magnetic B_z component during the QRS complex at the front side of the thorax (1isoline=2pT).

4 Discussion

The magnetic field can provide additional important details about properties of the field sources which are not recognizable in the electrical potential on the body surface especially if curved or circular currents are involved. The electrical potential at the surface depends on the electrical strength and consequently only on the conductivity and the volume currents close to the body surface. In contrary, in the case of the magnetic field, due to the whole current distribution and especially curved current sources and volume parts with high current density we can observe a regionally focused magnetic flux. We suggest to interpret such field measurements in terms of curved current structures. Further studies should clarify more detailed electrophysiological correlates for such curved current structures

Acknowledgements

This work was supported by the BMBF in the project 01Kx9912/8.

References

1. P.C. Franzone, L. Guerri, M. Pennacchio and B. Taccardi, „Spread of excitation in 3-D models of the anisotropic cardiac tissue. II. Effects of fiber architecture and ventricular geometry“, *Math Biosci*, 147 **(2)**, 131–171 (1998).
2. H. Brauer et. al., „Investigation of Biomagnetic Source Reconstruction Methods Using Realistic Thorax Phantoms“, *Biomed Tech*, 42 **(1)**, 99-102, (1997).
3. M. Burghoff, W. Haberkorn, B.-M. Mackert, G. Curio and L. Trahms, “Modellierung und Analyse von ausgedehnten Stromquellen: Das Magnetfeld von stimulierten peripheren Nerven”, *Biomed Tech*, 43 **(1)**, 224-225, (1998).
4. V. Jazbinsek, O. Kosch, P. Meindl, U. Steinhoff and L. Trahms, “Multichannel vector MFM and BSPM of chest and back”, in this proceedings.